JOURNAL OF GUIDANCE, CONTROL, AND DYNAMICS
Vol. 22, No. 5, September–October 1999

Classification of Out-of-Plane Swing-By Trajectories

Gislaine de Felipe* and Antonio Fernando Bertachini de Almeida Prado†
National Space Research Institute, 12227-010 São Josè dos Campos, Brazil

The swing-by maneuver uses a close approach with a celestial body to modify the velocity, energy, and angular momentum of a spacecraft. The literature has several papers studying this problem, usually using a patched-conic approximation. In the present paper the swing-by maneuvers are studied and classified under the model given by the three-dimensional restricted three-body problem. To show the results, the orbits of the spacecraft are classified in four groups: elliptic direct, elliptic retrograde, hyperbolic direct, and hyperbolic retrograde. Then the modification in the orbit of the spacecraft caused by the close approach is shown in plots that specify from which group of orbits the spacecraft is coming and to which group it is going. Several families of orbits are found and shown in detail. The effect of every parameter involved in this problem is studied individually. The results generated here have a potential use to solve optimal problems, such as finding trajectories that satisfy some given constraints (such as achieving an escape or capture) with some parameters being extremized (position, velocity, etc.). Two optimal problems are solved in this paper to show this application.

Nomenclature

C_z	= Z component of the angular momentum
C_+	= angular momentum after the encounter
C_-	= angular momentum before the encounter
E_+	= energy after the encounter
E_-	= energy before the encounter
J	= Jacobian constant
M_1	= primary body
M_2	= secondary body
m_1	= real mass of the primary body
m_2	= real mass of the secondary body
P	= point of the closest approach
r_p	= distance of the spacecraft at periapse
r_1	= distance of the spacecraft from M_1
r_2	= distance of the spacecraft from M_2
V_{inf}	= velocity at infinite
v_p	= velocity of the spacecraft at periapse
V_{xi}, V_{yi}, V_{zi}	= initial velocity of the spacecraft
V_2	= linear velocity of M_2
X_i, Y_i, Z_i	= initial position of the spacecraft
x, y, z	= position of the spacecraft
x_1, y_1	= position of M_1
x_2, y_2	= position of M_2
α	= angle specified in Fig. 1
β	= out-of-plane angle (see Fig. 1)
γ	= angle between the velocity vector and the x–y plane
ΔC	= variation in angular momentum
ΔE	= variation in energy
ΔV	= variation in velocity
δ	= half of the deflection angle
μ	= gravitational parameter
μ_2	= gravitational parameter of M_2
ω	= angular velocity of the primaries

Introduction

THE swing-by maneuver is a very popular technique used to decrease fuel expenditure in space missions. The most usual approach to study this problem is to divide the problem in three phases dominated by the two-body celestial mechanics. Other models used to study this problem are the circular restricted three-body problem[1–3] and the elliptic restricted three-body problem.[4]

In the present paper the swing-by maneuvers are studied and classified under the model given by the three-dimensional circular restricted three-body problem. The assumption is made that the system is formed by two main bodies that are in circular orbits around their center of mass and a massless third body that is moving under the gravitational attraction of the two primaries.

The goal is to simulate a large variety of initial conditions for those orbits and classify them according to the effects caused by the close approach in the orbit of the spacecraft. This swing-by is assumed to be performed around the secondary body of the system. Special attention is given to identify the regions where the captures and escapes occur.

Among the several sets of initial conditions that can be used to identify uniquely one swing-by trajectory, a modified version of the set used in Refs. 1–3 is used here. The version is composed of the following four variables: 1) v_p, the velocity of the spacecraft at periapse of the orbit around the secondary body; 2) two angles α and β that specify the direction of the periapse of the trajectory of the spacecraft around M_2 in a three-dimensional space; and 3) r_p, the distance from the spacecraft to the center of M_2 in the moment of the closest approach to M_2 (periapse distance).

For a large number of values of these three variables, the equations of motion are integrated numerically forward and backward in time until the spacecraft is at a distance that can be considered far enough from M_2. It is necessary to integrate in both directions of time because the set of initial conditions used gives information about the spacecraft exactly at the moment of the closest approach. At these two points the effect of M_2 can be neglected and the system formed by M_1 and the spacecraft can be considered a two-body system. At these two points two-body celestial mechanics formulas are valid to compute the energy and the angular momentum before and after the close approach. With those results the orbits are classified in four categories: elliptic direct (negative energy and positive angular momentum), elliptic retrograde (negative energy and angular momentum), hyperbolic direct (positive energy and angular momentum), and hyperbolic retrograde (positive energy and negative angular momentum). Then, the problem is to identify the category of the orbit of the spacecraft before and after the close encounter with M_2. After that those results are used to identify up to 16 classes of transfers, accordingly to the changes in the category of the orbit caused by the close encounter. They are named with the first 16 letters of the alphabet.

Using a large number of simulations, it is possible to understand the influence of each parameter and improve our understanding of this problem. Also, several optimal problems involving this maneuver can be formulated and solved with the help of the plots shown.

Received 11 March 1998; revision received 16 March 1999; accepted for publication 16 April 1999.

*Post Graduate Student; gislaine@dem.inpe.br.

†Research Engineer, Space Mechanics and Control Division; prado@dem.inpe.br. Senior Member AIAA.

Some examples include finding specific types of orbits (escape, capture, etc.) that have maximum or minimum velocity at periapsis (or any other parameters, such as the distance of the periapsis or the angle of approach). A section of this paper shows some of the possibilities.

Several papers were written in the past on this subject. References 5–7 are among the most interesting ones.

Swing-By in Three Dimensions

The three dimensional swing-by maneuver consists of using a close encounter with a celestial body to change the velocity, energy, and angular momentum of a smaller body (a comet or a spacecraft). This maneuver can be identified by four independent parameters:

1) v_p is the magnitude of the velocity of the spacecraft at periapse. For the most general case, one would need to give information about the direction of the velocity. In this paper only velocities parallel to the x–y plane are considered with the exeption of a section in the end of the paper that generalizes this initial condition. This constraint is assumed because it is the most usual situation in interplanetary research and because the planets have orbits that are almost coplanar. Under this approximation, and taking into account that velocity at periapse is perpendicular to the periapse vector, the information about the magnitude of the velocity is enough to completely specify the velocity vector.

2) r_p is the distance between the spacecraft and the celestial body during the closest approach.

3) α is the angle between the projection of the periapse line in the x–y plane and the line that connects the two primaries.

4) β is the angle between the periapse line and the x–y plane.

Figure 1 shows the sequence for this maneuver and some of those and other important variables.

The assumption is made that the system has three bodies: a primary M_1 and a secondary M_2 body with finite masses that are in circular orbits around their common center of mass and a third body with negligible mass (the spacecraft) that has its motion governed by the two other bodies. The spacecraft leaves the point A, passes by the point P (the periapsis of the trajectory of the spacecraft in its orbit around M_2), and goes to the point B. The points A and B are chosen in a such way that the influence of M_2 at those two points can be neglected, and, consequently, the energy can be assumed to remain constant after B and before A (the system follows the two-body celestial mechanics). The initial conditions are clearly identified in Fig. 1: the perigee distance r_p (distance measured between the point P and the center of M_2), the angles α and β, and the velocity v_p. The distance r_p is not to scale, to make the figure easier to understand. The result of this maneuver is a change in velocity, energy, and angular momentum in the Keplerian orbit of the spacecraft around the central body. Using the patched conic approximation, the equations that quantify those changes are available in the literature.[1] Under this approximation the maneuver is considered as composed of three parts, where each of those systems are governed by the two-body celestial mechanics. The first system describes the motion of the spacecraft around the primary body before the close encounter (the secondary body is neglected). When the spacecraft comes close to the secondary body, the primary is neglected, and a second two-body system is formed by the spacecraft and the secondary body. After the close encounter the spacecraft leaves the secondary body, and it goes to an orbit around the primary body again. Then, the secondary is neglected one more time. One of the best descriptions of this maneuver and the derivation of the equations involved is available in Ref. 1. The most important equations for the planar maneuver are reproduced next.

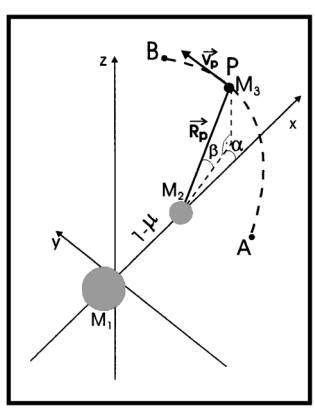

Fig. 1 Swing-by in the three-dimensional space.

$$\delta = \sin^{-1}\left[1 \Big/ \left(1 + \frac{r_p V_{\text{inf}}^2}{\mu_2}\right)\right] \tag{1}$$

$$\Delta V = 2V_{\text{inf}} \sin\delta \tag{2}$$

$$\Delta E = \omega \Delta C = -2V_2 V_{\text{inf}} \sin\delta \sin\alpha \tag{3}$$

In those equations δ is half of the total deflection angle of the trajectory of the spacecraft, V_2 is the linear velocity of M_2 in its motion around the center of mass of the system M_1–M_2, and μ_2 is the gravitational parameter of M_2. From those equations it is possible to get the fundamental well-known results:

1) The variation in energy ΔE is equal to the variation in angular momentum multiplied by the angular velocity of the primaries ($\omega \Delta C$) [Eq. (3)].

2) If the flyby is in front of the secondary body, there is a loss of energy. This loss has a maximum at $\alpha = 90$ deg.

3) If the flyby is behind the secondary body, there is a gain of energy. This gain has a maximum at $\alpha = 270$ deg.

Equations (1–3) use V_{inf} as a parameter. Later in this paper the variable v_p will be used. The fact is that both parameters are equivalent because the orbit around M_2 is considered Keplerian (hyperbolic) in the approximation used to derive those equations (patched conics). They are related by the expression

$$V_{\text{inf}}^2 = v_p^2 - (2\mu/r_p)$$

There are many publications studying the standard swing-by maneuver in different missions. Some examples are as follows: the study of missions to the satellites of the giant planets,[8] new missions to Neptune[9] and Pluto,[10] the study of the Earth's environment,[11,12] fast reconnaissance missions of the solar system,[13,14] transfers between hyperbolic asymptotes,[15,16] etc.

Three-Dimensional Circular Restricted Problem

For the research performed in this paper, the equations of motion for the spacecraft are assumed to be the ones valid for the well-known three-dimensional restricted circular three-body problem. The standard dimensionless canonical system of units is used, which implies that the unit of distance is the distance between M_1 and M_2; the mean angular velocity ω of the motion of M_1 and M_2 is assumed to be one; the mass of the smaller primary M_2 is given by $\mu = m_2/(m_1 + m_2)$, where m_1 and m_2 are the real masses of M_1 and M_2, respectively; and the mass of M_2 is $(1 - \mu)$; and the unit of time is defined such that the period of the motion of the two primaries is 2π and the gravitational constant is one.

There are several systems of reference that can be used to describe the three-dimensional restricted three-body problem.[17] In this paper the rotating system is used.

In the rotating system of reference, the origin is the center of mass of the two massive primaries. The horizontal axis x is the line that connects the two primaries at any time. It rotates with a variable angular velocity in a such way that the two massive primaries are always on this axis. The vertical axis y is perpendicular to the x axis. In this system the positions of the primaries are $x_1 = -\mu, x_2 = 1 - \mu$, and $y_1 = y_2 = 0$.

In this system the equations of motion for the massless particle are the following[17]:

$$\ddot{x} - 2\dot{y} = x - (1-\mu)\frac{x+\mu}{r_1^3} - \mu\frac{x-1+\mu}{r_2^3} \tag{4}$$

$$\ddot{y} + 2\dot{x} = y - (1-\mu)\left(y/r_1^3\right) - \mu\left(y/r_2^3\right) \tag{5}$$

$$\ddot{z} = -(1-\mu)\left(z/r_1^3\right) - \mu\left(z/r_2^3\right) \tag{6}$$

where r_1 and r_2 are the distances from M_1 and M_2.

Algorithm to Solve the Problem

A numerical algorithm to solve the problem has the following steps:

1) Arbitrary values for the three parameters r_p, v_p, α and β are given.

2) With these values the initial conditions in the rotating system are computed. The initial position is the point (X_i, Y_i, Z_i) and the initial velocity is (V_{Xi}, V_{Yi}, V_{Zi}), where

$$X_i = 1 - \mu + r_p \cos(\beta) \cos(\alpha) \tag{7}$$

$$Y_i = r_p \cos(\beta) \sin(\alpha) \tag{8}$$

$$Z_i = r_p \sin(\beta) \tag{9}$$

$$V_{Xi} = -v_p \sin(\alpha) + r_p \cos(\beta) \sin(\alpha) \tag{10}$$

$$V_{Yi} = v_p \cos(\alpha) - r_p \cos(\beta) \cos(\alpha) \tag{11}$$

$$V_{Zi} = 0 \tag{12}$$

where the last equation comes from the decision of studying the maneuvers with v_p parallel to the orbital plane of the primaries.

3) With these initial conditions the equations of motion are integrated forward in time until the distance between M_2 and the spacecraft is larger than a specified limit d. At this point the numerical integration is stopped, and the energy E_+ and the angular momentum C_+ after the encounter are calculated.

4) Then, the particle goes back to its initial conditions at the point P, and the equations of motion are integrated backward in time until the distance d is reached again. Then the energy E_- and the angular momentum C_- before the encounter are calculated.

For all of the simulations shown, a fourth-order Runge–Kutta method with step-size control and a Runge–Kutta of eighth order were used for numerical integration. The result of this comparison is that there is no distinction in the plots obtained. The constant value for the Jacobian constant also is a proof that both numerical integration methods worked very well. The criteria to stop numerical integration is the distance between the spacecraft and M_2. When this distance reaches the value $d = 0.5$ (half of the semimajor axis of the two primaries), the numerical integration is stopped. The value 0.5 is a lot larger than the sphere of influence of M_2 for the Earth–moon system that is used here (which is 0.00077 in canonical units), which avoids any important effects of M_2 at these points. Simulations using larger values for this distance were performed that increased the integration time but did not significantly change the results. To study the effects of numerical accuracy, several cases were simulated using different integration methods and/or different values for the accuracy required with no effects in the results. All of the calculations were performed with an IBM-PC computer (Pentium 233MHz) using the Microsoft Fortran Power Station 4.0 Compiler.

With this algorithm available the given initial conditions (values of r_p, v_p, α, β) are varied in any desired range, and the effects of the close approach in the orbit of the spacecraft are studied.

Classification of the Orbits

The main results consist of plots that show the change of the orbit of the spacecraft caused by the close encounter with M_2. The Earth–moon system of primaries is used because it has many potential applications. Any mission using a swing-by with the moon can use those results, like missions to the moon using gravitational capture or mission to geosynchronous orbit using the concept used by the salvage of the mission. First of all, one needs to classify all of the close encounters between M_2 and the spacecraft, according to the change obtained in the orbit of the spacecraft. The letters A–P are used for this classification. They are assigned to the orbits according to the rules showed in Table 1.

With those rules defined, the results consist of assigning one of those letters to a position in a two-dimensional diagram that has the angle α (in degrees) in the horizontal axis and the angle β (in degrees) in the vertical axis. One plot is made for every value of r_p and v_p. This type of diagram is called here a letter-plot and was used before in Ref. 1.

Table 1 Rules to assign letters to orbits

Before	After: Direct ellipse	Retrograde ellipse	Direct hyperbola	Retrograde hyperbola
Direct ellipse	A	E	I	M
Retrograde ellipse	B	F	J	N
Direct hyperbola	C	G	K	O
Retrograde hyperbola	D	H	L	P

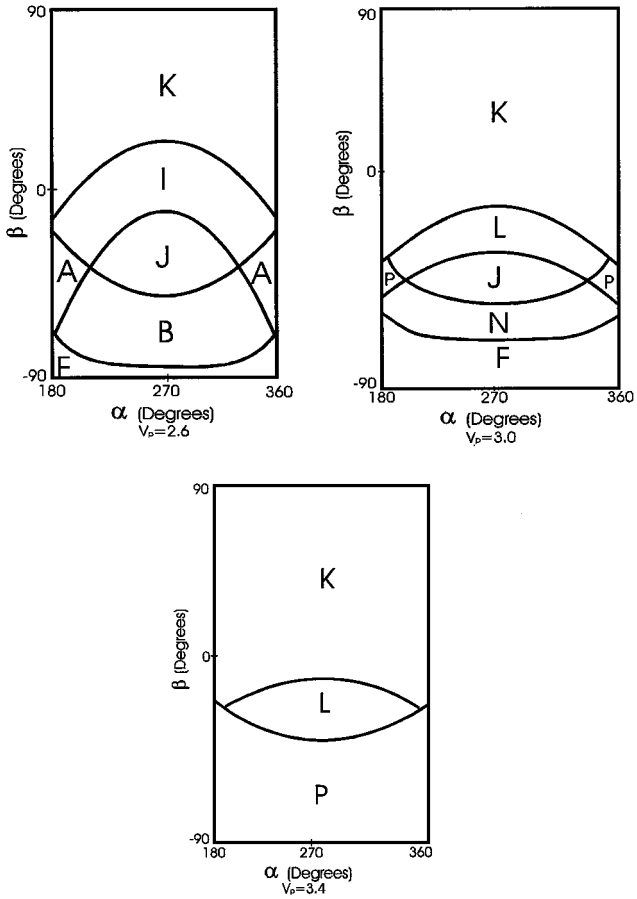

Fig. 2 Simulations for $r_p = 0.00476$.

In the present paper 12 combinations r_p and v_p are simulated and six of them are shown in Figs. 2 and 3. The plot for $r_p = 0.00476$ and $v_p = 2.2$ is omitted here because of the large number of captures by M_2 that occur. The plots for $r_p = 0.00675$ are omitted here to save space because they are similar to the other cases. For all plots the following parameters are used: $\mu = 0.0121$ and $d = 0.5$, all in canonical units. For each plot a total of 961 trajectories were generated, dividing each axis in 31 segments. The interval plotted for α is $180 < \alpha < 360$ deg because there is a symmetry with respect to the vertical line $\alpha = 180$ deg. The plot for the interval $0 < \alpha < 180$ deg is a mirror image of the region $180 < \alpha < 360$ deg with the following letter substitutions: L becomes O, N becomes H, I becomes C, B becomes E, M becomes D, and J becomes G. The letters K, P, F, and A remain unchanged.

By examining Figs. 2 and 3, it is possible to identify the following families of orbits: 1) orbits that result in an escape (transfer from elliptic to hyperbolic), that are represented by the letters I, J, M, N, and that appear between the center ($\beta = 0$ deg) and the bottom part of some of the plots (the ones for lower velocities); 2) orbits that result in a capture (transfer from hyperbolic to elliptic), that are represented by the letters C, D, G, H, and that do not appear in the plots shown in this paper (but exist in the symmetric part not shown here); 3) elliptic orbits (transfer from elliptic to elliptic) that are represented by the letters A, B, E, F, and that appear at the bottom of some of the plots (the ones for lower velocities); 4) hyperbolic

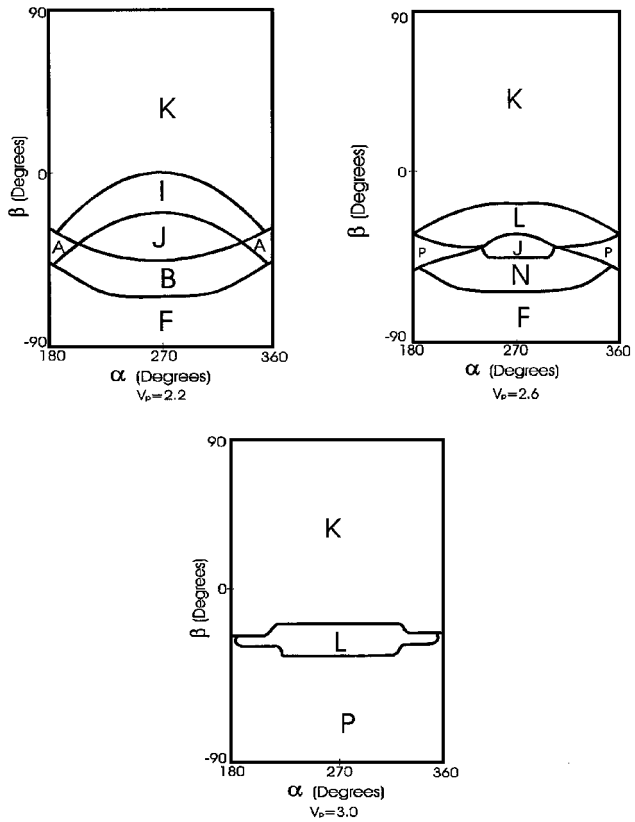

Fig. 3 Simulations for $r_p = 0.009$.

orbits (transfer from hyperbolic to hyperbolic) that are represented by the letters K, L, O, P and that appears at the upper part of the plots, and that are the only families available for higher velocities; 5) orbits that change the direction of motion from direct to retrograde that are represented by the letters E, M, G, O, and that do not appear in the plots shown in this paper (but exist in the symmetric part not shown here); 6) orbits that change the direction of motion from retrograde to direct, that are represented by the letters B, D, J, L, and that appear in the lower center of the plot; 7) retrograde orbits that are represented by the letters F, H, N, P and that appear in the majority of the bottom part of the plots; and 8) direct orbits that are represented by the letters A, C, I, K that appear in the top of the plots.

The border lines between those families are also interesting families of orbits. The borders that separate elliptic from hyperbolic orbits are made by parabolic orbits. Examples of borders that have parabolic orbits after the close approach are A-I, B-J, F-N, F-J, and F-P. Examples of borders that have parabolic orbits before the close approach are I-K, J-L, N-P, K-A, K-J, and F-P. There is a border that is made by parabolic orbits before and after the close approach. It is the border P-F that appears, for example, in the case $r_p = 0.009$ and $v_p = 2.6$. The borders that separate direct from retrograde orbits are made of orbits with zero angular momentum, which means that the vectors position and velocity are parallel (rectilinear orbits). Examples of borders that have zero angular momentum after the close approach are F-B, N-J, L-P, P-K, N-L, and F-A. Examples of borders that have zero angular momentum before the close approach are K-L, I-J, A-B, K-P, and K-J. Following those examples, one can see those families looking at the figures.

The goal of this research is to provide a generic study of those trajectories, using the position and velocity of the spacecraft during the moment of the close approach as parameters to be varied in a wide range of values. Figures 2 and 3 shows plots with $r_p = 0.00476$ (100 km above the surface of the moon) and $r_p = 0.009$ (3500 km above the surface of the moon). Some of the important points to note in the figures are that 1) positive values of β are dominated by the family K in all cases (hyperbolic orbits), while negative values accommodate a large variety of families; 2) for a fixed value of r_p the increase of the velocity reduces the number of families, which has a tendency to be formed by the families K, L, and P (hyperbolic orbits) exclusively; and 3) when r_p increases the minimum velocity required for this to happen also increases.

The Jacobi constant was calculated for all of the trajectories involved. Among the several forms available in the literature, the expression

$$J = \frac{V^2}{2} - \frac{(x^2 + y^2)}{2} - \frac{(1-\mu)}{r_1} - \frac{\mu}{r^2}$$

was used. Each point in the plots shown represents one trajectory and has its own value for the Jacobi constant. The ranges of values are $-0.6378 < J < 1.7621$ for Figs. 2 and 3.

Trends as Parameters Vary

The restricted three-body problem has very few analytical results available in the literature. One of the best alternatives for improving the knowledge of this problem is to combine numerical simulations with the analytical results that come from the patched-conic approximation. In this section those tools are used to study the trends as parameters vary in the close approach maneuver.

The parameters that govern the system under study are the periapsis distance r_p, the velocity at periapsis v_p, and the angles α and β that define the position of the periapsis in the three-dimensional space.

Effects of the Angle of Approach r_p

The behavior of the angle of approach α follows very closely[1] the prediction of the patched-conic approximation. The maximum effect in the maneuver occurs close to $\alpha = 270$ deg (and $\alpha = 90$ deg). The most interesting trajectories (captures and escapes) are in those regions. Close to the borders of the plots ($\alpha = 180$ and 360 deg), there are only trajectories with little or no effects from the swing-by (elliptic–elliptic and hyperbolic–hyperbolic). The angle α also has an influence on the definition of the type of the orbit. Following a line of constant β (so all of the parameters are fixed, except α), the initial orbit is not of the same type.

Effects of the Periapsis Distance r_p

The effect of the periapsis distance is also very easy to understand. When this parameter decreases, the effects in the maneuver increase, and the area of interesting orbits (captures/escapes) becomes larger. Conversely, increasing the periapsis distance increases the area of trivial trajectories (elliptic–elliptic, hyperbolic–hyperbolic, etc.). Several simulations (not shown here, to save space) were performed and confirmed this prediction.

Effects of the Periapsis Velocity

The velocity at periapsis plays an important role in this maneuver. The limits for this variable come in a very natural way. If values above an upper limit are used, the ΔE increases [see Eq. (3)], but the orbit before and after the maneuver becomes hyperbolic and the families K, P, and L dominate the plots. Those limits change from situation to situation, but in general they are close to 2.20 in the lower side and 3.40 in the upper side. For values slightly above the lower limit, the orbits are usually elliptic before and/or after the maneuver, as the families A, B, F, J, and I that dominate the bottom part of the plots. There is a minimum value for this velocity that allows a change in the sign of the angular momentum.

Effects of the Out-of-Plane Angle β

The study of the effects of the out-of-plane angle β is one of the main goals of this paper. To study this effect, one must look at vertical lines in the plots because they represent the places where all of the other parameters are fixed.

For values for the velocity close to the upper limit used in this paper, the analysis of the effect of β becomes very simple. The only three families available are K, L, and P, and they are strongly dependent on β. It is formed by hyperbolic orbits before and after the close encounter. The effect of β can be summarized in the following way: 1) if $\beta > 0$, it implies that there is a direct orbit before and after

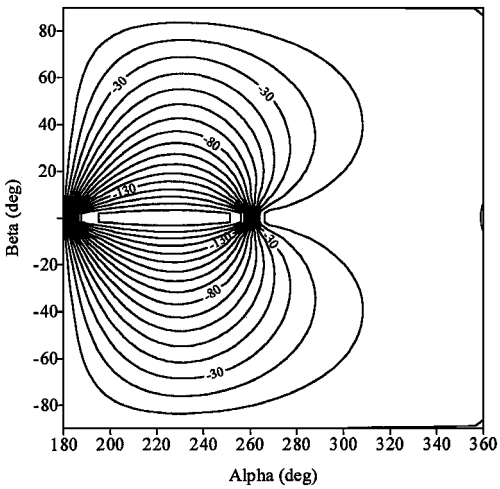

Fig. 4 Results for delta inclination.

the maneuver (family K); 2) if β is approximately between zero and -30 deg, the swing-by will change the orbit from retrograde to direct orbits; and 3) if β is less than approximately -30 deg, this implies that the orbit is retrograde before and after the approach. This result is expected because trajectories close to the poles ($\beta \cong \pm 90$ deg) have a small effect in changing direction.

Effects on the Inclination

An interesting question that appears in this problem is what happens to the inclination of the spacecraft because of the close approach. To investigate this fact, the inclinations of the trajectories were calculated before and after the closest approach. To obtain the inclinations, the equation $\cos(i) = C_z/C$ is used, where C_z is the Z component of the angular momentum and C is the total angular momentum. Figure 4 shows the results for the case given by the initial conditions $v_p = 2.6$, $r_p = 0.00476$, and $\mu = 0.0121$. The horizontal axis represents the angle α, and the vertical axis represents the angle β. The variation in inclination is shown in the contour plots. All of the angles are expressed in degrees.

Several conclusions come from those results. The most interesting ones are the following:

1) When $\beta = 0$ deg (planar maneuver), the variation in inclination can have only three possible values: ± 180 deg, for a maneuver that reverse the sense of its motion, or 0 deg for maneuver that does not reverse its motion. Those numerical results agree with the physical model because $\beta = 0$ deg implies a planar maneuver that does not allow values for the inclination other than 0 or 180 deg. This is clearly shown in the figures, following the line $\beta = 0$ deg. The plots are divided in two parts: one with $\Delta i = \pm 180$ deg, and the other one with $\Delta i = 0$ deg.

2) Looking at any vertical line (a line of constant α), it is clear that the change in inclination goes to zero at the poles ($\beta = \pm 90$ deg). Then, in the case where $\Delta i = \pm 180$ deg the change in inclination starts at zero in $\beta = -90$ deg, increases in magnitude until $\beta = 0$ deg, and then it starts decreasing again until zero when $\beta = 90$ deg is reached. When $\Delta i = 0$ deg for $\beta = 0$ deg, the behavior of Δi oscillates with two maximum for the magnitude (one in the interval -90 deg $< \beta < 0$ deg) and the other in the interval 0 deg $< \beta <$ 90 deg) and three zeros at $\beta = -90$, 0, 90 deg. Clearly the variation in inclination is symmetric with respect to the angle β ($+\beta$ and $-\beta$ generate the same Δi).

3) When $\beta = \pm 90$ deg, the variation in inclination is zero, which means that passage by the poles with the velocity parallel to the x–y plane (this restriction will be changed later, but it is valid at this point) keeps the inclination of the trajectory unchanged.

4) When $\alpha = 0$ or 180 deg, there is no change in the inclination, which is in agreement with the fact that a maneuver with this geometry does not change the trajectory at all. Looking at any horizontal line (a line of constant β), this curve has a maximum in the magnitude of Δi somewhere between the two fixed zeroes at $\alpha = 0$ and 180 deg.

Effects of the Out-of-Plane Velocity at Periapsis

In this section a generalization is made to the velocity at periapis to allow an out-of-plane component. To perform this study, an angle γ is added to the geometry. This angle is measured between the velocity at periapse and the x–y plane. Then, the initial conditions for the velocity [Eqs. (10–12)] change to

$$V_{Xi} = -v_p \sin(\gamma)\sin(\beta)\cos(\alpha) - v_p \cos(\gamma)\sin(\alpha) + r_p \cos(\beta)\sin(\alpha) \tag{13}$$

$$V_{Yi} = -v_p \sin(\gamma)\sin(\beta)\sin(\alpha) + v_p \cos(\gamma)\cos(\alpha) - r_p \cos(\beta)\cos(\alpha) \tag{14}$$

$$V_{Zi} = v_p \cos(\beta)\sin)(\gamma) \tag{15}$$

The initial conditions for the positions [Eqs. (7–9)] remain unchanged.

To study the influence of this angle in the maneuver, the variations in energy and angular momentum were calculated and plotted in Fig. 5 as a function of γ. The variation in inclination is shown in Fig. 6. The numerical conditions for this plots are $\alpha = 20$ deg, $\beta = 0$ deg, and $\mu = 0.0121$. Simulations with other values were

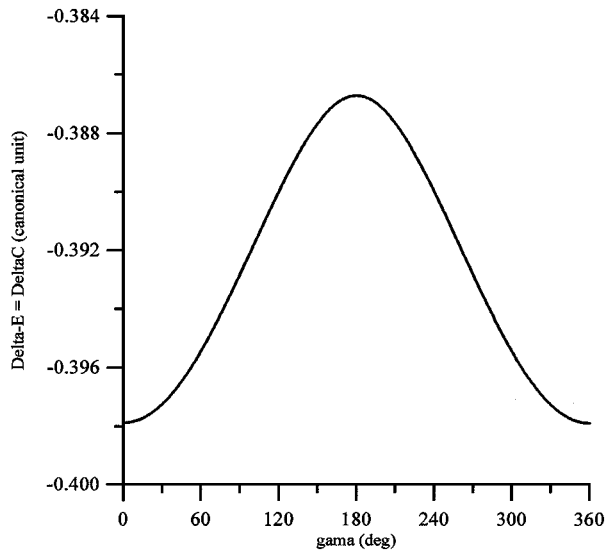

Fig. 5 $\Delta E = \Delta C$ vs γ.

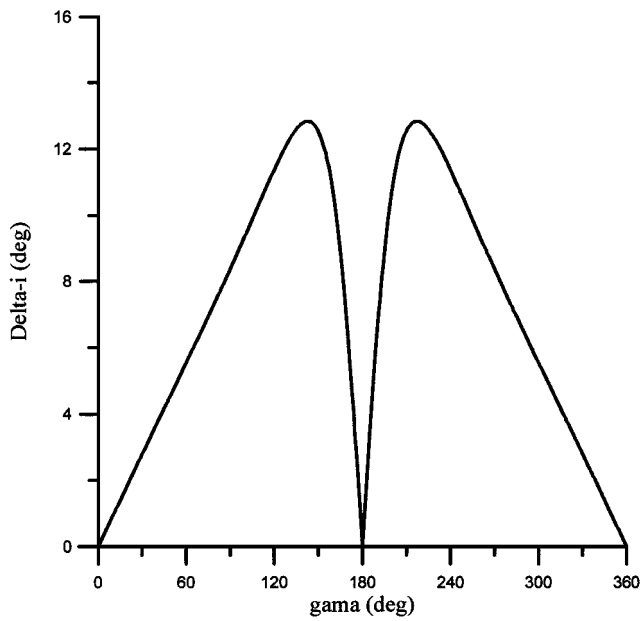

Fig. 6 Δi vs γ.

made with similar results, but are not shown here because of the limitation of space. The results show that this angle plays a very important rule in the maneuver. The variation in energy has a maximum for $\gamma = 180$ deg and minimum in $\gamma = 0$ and 360 deg. The variation in inclination has a simmetry line in $\gamma = 180$ deg. There are two maximums close to $\gamma = 150$ and 210 deg.

Optimal Problems

The results generated in this research can be used to help mission designers plan missions that involve optimization of parameters. It is possible to use the plots made here to find situations where a specific case (represented by the letters A–P) can be obtained with one or more variables (like v_p or r_p) extremized. Examples of situations like that are 1) finding a trajectory N (a retrograde ellipse before the swing-by and a retrograde hyperbola after that) that has a fixed r_p and that minimizes the parameter v_p; 2) finding a trajectory E, F, G, or H (a retrograde ellipse after the swing-by) that has a fixed r_p and that maximizes the parameter v_p; and 3) finding a trajectory of type L (retrograde hyperbola before and a direct hyperbola after the swing-by) that has r_p and v_p fixed and that extremizes the parameters α or β.

The parameters v_p and r_p are important parameters to be extremized. If the goal of the mission is to collect data from M_2, it is interesting to minimize r_p (to get closer to M_2) and v_p (to stay closer to M_2). On the other hand, if M_2 is necessary to be used to change the trajectory of the spacecraft but it represents a risk to the vehicle because of the presence of an atmosphere and/or radiation, one needs to maximize r_p and/or v_p, subject to the restriction of obtaining the desired change in the trajectory. To use a real case as an example, the Earth–moon system is used to solve the two sample problems that are described next.

Problem 1

We want to obtain a trajectory of type J (a retrograde ellipse before the swing-by and a direct hyperbola after) in the Earth–moon system, subject to the constraints $r_p = 0.00476$ (100 km above the surface) and requiring that the velocity at periapsis be a maximum. By examining Fig. 2, one can to see that the trajectory type J appears for $v_p = 3.0$, but does not appear for $v_p = 3.4$. The solution is somewhere in the interval $3.0 < v_p < 3.4$. To find the solution, plots were made for several values of v_p in this interval. Figure 7 shows two plots of this sequence. The solution to this problem is $v_p = 3.15$ because for $V_p = 3.16$ J does not occur anymore. The complete values for the set of variables are $\alpha = 270$ deg and $\beta = -42$ deg.

Problem 2

We want to find a trajectory of type N (a retrograde escape) in the Earth–moon system, subject to the constraints $v_p = 3.0$ and requiring that r_p is maximized. By examining Figs. 2 to 3, one can see that the trajectory type N, in the case $v_p = 3.0$, appears for $r_p = 0.00476$ and $r_p = 0.00675$, but does not appear for $r_p = 0.009$. The solution is in the interval $0.00675 < r_p < 0.009$. Figure 8 shows two plots of the sequence made to find the solution. The solution to this problem

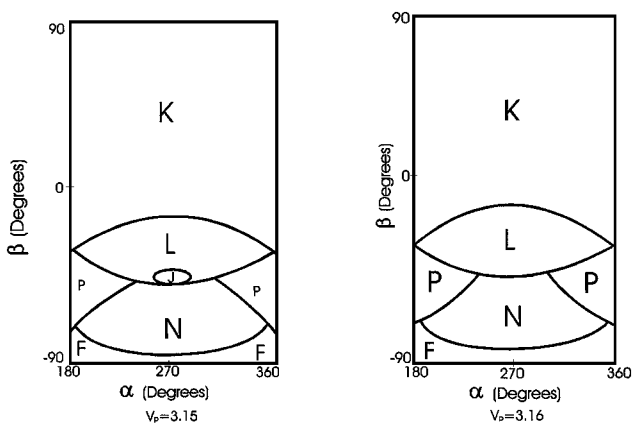

Fig. 7 Plots to solve problem 1.

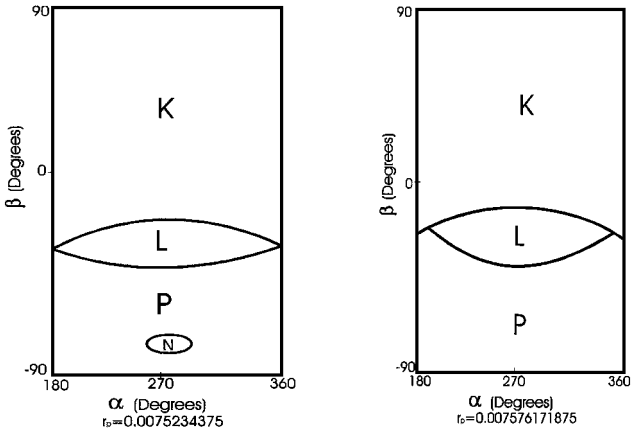

Fig. 8 Plots to solve problem 2.

is $r_p = 0.0075234375$. The complete values for the set of variables are $\alpha = 270$ deg and $\beta = -78$ deg. This information constitutes a set of initial conditions that allows the mission planner to design the trajectory.

Several improvements can be made in this study, including the following: 1) more plots can be generated to get more accuracy for the data, in particular in the solutions of the optimal problems; 2) many other types of optimization problems can be solved, combining different constraints and/or variable to be extremized; and 3) others systems than the Earth–moon can be used.

Conclusions

In this paper the three-dimensional restricted three-body problem is described and used to study the swing-by maneuver. Several letter-plot types of graphics are made to represent the effect of a close approach in the orbit of a spacecraft. In particular, the effects of the third dimension in this maneuver are studied. We have shown that the hyperbolic orbits (family K) dominate the region of positive β and that when the velocity increases, the families K, L, and P dominate the plots. Families with particularities, like parabolic or zero angular momentum orbits, are shown to exist in the borders between the main families. In general, one can clearly see that the third dimension of the maneuver plays a very important role in the problem under investigation. To make this research more adequate for practical applications, the results available here were used in two topics: 1) a study of the trends as parameters vary to show the effects of the angle of approach, periapse distance, periapse velocity, and out-of-plane angle; and 2) the solution of optimal problems, such as finding specific trajectories (escape, capture, etc.) that have constraints in some variable and that extremize some others, like the periapse distance and/or the velocity at the periapse. After that the effects of the close approach in the inclination of the spacecraft are studied, and the results show several particularities, like $\beta = 0$ deg allows only ± 180 and 0 deg for Δi and $\beta = \pm 90$ deg or $\alpha = 0$ or 180 deg implies $\Delta i = 0$ deg. The effects of an out-of-plane component for the velocity at periapse were also studied, and its importance was shown, changing the values for the variation in inclination, energy, and angular momentum, as described in the plots shown. In this way this research can be used by mission designers to obtain specific mission goals.

Acknowledgments

The authors are grateful to the National Council for Scientific and Technological Development (CNPq), Brazil, for the research grant received under Contracts 300221/95-9, and to the Foundation to Support Research in the São Paulo State (FAPESP) for the research grant received under Contracts 1995/9290-1 and 97/13739-0.

References

[1] Broucke, R. A., "The Celestial Mechanics of Gravity Assist," AIAA Paper 88-4220, Aug. 1988.

[2] Broucke, R. A., and Prado, A. F. B. A., "Jupiter Swing-By Trajectories Passing Near the Earth," *Space Flight Mechanics*, edited by R. G. Melton,

L. J. Wood, R. C. Thompson, and S. J. Kerridge, Advances in the Astronautical Sciences, Vol. 82, Pt. 2, Pasadena, CA, 1993, pp. 1159–1176.

[3]Prado, A. F. B. A., "Optimal Transfer and Swing-By Orbits in the Two- and Three-Body Problems," Ph.D. Dissertation, Dept. of Aerospace Engineering and Engineering Mechanics, Univ. of Texas, Austin, TX, Dec. 1993.

[4]Prado, A. F. B. A., "Close-Approach Trajectories in the Elliptic Restricted Problem," *Journal of Guidance, Control, and Dynamics*, Vol. 20, No. 4, 1997, pp. 797–802.

[5]Everhart, E., "Close Encounters of Comets and Planets," *The Astronautical Journal*, Vol. 74, No. 5, 1969, pp. 735–750.

[6]Newton, H. A., "On the Origin of Comets," *American Journal of Science and Arts*, Vol. 16, No. 93, 1878, pp. 165–179.

[7]Newton, H. A., "On the Capture of Comets by Planets, Especially Their Capture by Jupiter," *Memoirs of the National Academy of Sciences*, Vol. 6, No. 1, 1893, pp. 7–23.

[8]D'Amario, L. A., Byrnes, D. V., and Stanford, R. H., "Interplanetary Trajectory Optimization with Application to Galileo," *Journal of Guidance, Control, and Dynamics*, Vol. 5, No. 5, 1982, pp. 465–471.

[9]Swenson, B. L., "Neptune Atmospheric Probe Mission," AIAA Paper 92-4371, Aug. 1992.

[10]Weinstein, S. S., "Pluto Flyby Mission Design Concepts for Very Small and Moderate Spacecraft," AIAA Paper 92-4372, Aug. 1992.

[11]Farquhar, R. W., and Dunham, D. W., "A New Trajectory Concept for Exploring the Earth's Geomagnetic Tail," *Journal of Guidance, Control, and Dynamics*, Vol. 4, No. 2, 1981, pp. 192–196.

[12]Farquhar, R., Muhonen, D., and Church, L. C., "Trajectories and Orbital Maneuvers for the ISEE-3/ICE Comet Mission," *Journal of Astronautical Sciences*, Vol. 33, No. 3, 1985, pp. 235–254.

[13]Flandro, G., "Fast Reconnaissance Missions to the Outer Solar System, Utilizing Energy Derived from the Gravitational Field of Jupiter," *Astronautica Acta*, Vol. 12, No. 4, 1966, pp. 329–337.

[14]Carvell, R., "Ulysses—The Sun from Above and Below," *Space*, Vol. 1, No. 3, 1986, pp. 18–55.

[15]Gobetz, F. W., "Optimum Transfers Between Hyperbolic Asymptotes," *AIAA Journal*, Vol. 1, No. 9, 1963, pp. 2034–2041.

[16]Walton, J. M., Marchal, C., and Culp, R. D., "Synthesis of the Types of Optimal Transfers Between Hyperbolic Asymptotes," *AIAA Journal*, Vol. 13, No. 8, 1975, pp. 980–988.

[17]Szebehely, V., *Theory of Orbits*, Academic International, New York, 1967, Chap. 10.